Available online at www.sciencedirect.com
ScienceDirect
Ceramics International 34 (2008) 455–465
CERAMICS INTERNATIONAL
www.elsevier.com/locate/ceramint

Glass–ceramic frits for porcelain stoneware bodies: Effects on sintering, phase composition and technological properties

C. Zanelli [a,*], G. Baldi [b], M. Dondi [a], G. Ercolani [a], G. Guarini [a], M. Raimondo [a]

[a] CNR-Institute of Science and Technology for Ceramics, Via Granarolo 64, 48018 Faenza, Italy
[b] CERICOL, Colorobbia Research Centre, Via Pietramarina 123, 50053 Sovigliana Vinci, Italy

Received 22 March 2006; received in revised form 13 October 2006; accepted 14 November 2006
Available online 22 December 2006

Abstract

In the present work, the effects of glass–ceramic frits (10 wt.%) added to a porcelain stoneware body in replacement of non-plastic raw materials were evaluated simulating the tile-making process. Each glass–ceramic frit plays its own peculiar effect on the compositional properties and only some precursors behave as real glass–ceramic materials. The positive influence of glass–ceramic precursors in promoting the sintering stands out when temperature onset densification and sintering rate are considered: both of them are improved with respect to the reference body. The presence of glass–ceramic frits allows to preserve good technological properties, complying with the latest requirements of the industrial practice.

Keywords: A. Sintering; D. Glass ceramics; Ceramic tiles; Porcelain stoneware

1. Introduction

Porcelain stoneware tiles are characterized by a very low water absorption (<0.5% according to standard ISO 13006; <0.2% in current production) and excellent mechanical, tribological and functional properties for a building material [1–5].

Porcelain stoneware is a glass-bonded material manufactured in large size (up to 1 m^2) with fast cycles and a wide range of decorative techniques in order to bestow outstanding aesthetical effects [6].

Therefore, pressing exigencies for the tile-making industry are: (a) enhancing the sintering kinetics; (b) actually controlling firing shrinkage to achieve a uniform densification; (c) keeping adequate mechanical strength in large size tiles; (d) obtaining colour of fired stoneware as lightest as possible. In fact, ceramic pigments used to decorate porcelain stoneware present a relevant cost; a light-coloured body, especially if even translucent, allows to lower significantly the amount of pigment necessary to get the desired coloration [7].

In order to fulfil these exigencies, some kinds of glass–ceramic materials have, in the latest years, come in a wide use in porcelain stoneware production. They are vitreous precursors, prepared like ceramic frits, that are expected to devetrify during the fast firing cycle of the tile-making industry (typically 50–60 min cold-to-cold, with heating rates up to 80 °C/min and cooling rate up to 110 °C/min, maximum temperature 1200–1240 °C for 5–10 min soaking). The glass–ceramic systems entered in use are silicate and alumino-silicate of Na, Mg, K, Ca, Zn, Ba and Zr, though some further components may be present in the most complex formulations [7–19].

The effects played by these glass–ceramic frits in the firing process have been essentially studied by the technological viewpoint [20–25]. The role of glass–ceramic precursors on sintering kinetics, phase transformations and microstructure of porcelain stoneware is still to a large extent unknown.

The aim of the present paper is to fill this gap by investigating the firing behavior of seven glass–ceramic systems. The rationale is to introduce each frit in a typical porcelain stoneware body, simulating the industrial manufacturing in controlled laboratory conditions and assessing the changes induced by the glass–ceramic precursors on sintering and technological behaviour as well as microstructure and phase composition.

* Corresponding author. Tel.: +39 0546 699738; fax: +39 0546 46381.
E-mail address: czanelli@istec.cnr.it (C. Zanelli).

0272-8842/$34.00
doi:10.1016/j.ceramint.2006.11.008

Table 1
The glass–ceramic systems

Glass–ceramic frits	System	Component	Crystalline phases detected after devetrification
F0	CMAS	$CaO–MgO–Al_2O_3–SiO_2$	Anorthite, diopside and quartz
F1	ZCS	$CaO–ZrO_2–SiO_2$	Calcium zircosilicate, wollastonite and baddeleyite
F2	MAS	$MgO–Al_2O_3–SiO_2$	Indialite, forsterite, quartz, spinel and periclase
F3	BAS	$BaO–Al_2O_3–SiO_2$	Celsian
F4	NAS	$Na_2O–Al_2O_3–SiO_2$	Nepheline
F5	MAKZCS	$MgO–Al_2O_3–K_2O–ZrO_2–CaO–SiO_2$	Diopside, anorthite and baddeleyite
F6	CZnNAS	$CaO–ZnO–SiO_2–Na_2O–Al_2O_3$	Gahnite and plagioclase

Table 2
Physical properties of the glass–ceramic frits

Glass–ceramic frits	Bulk density (g cm^{-3})	Coefficient of thermal expansion (MK^{-1})	Temperature (°C) at log $\eta = 3$ (η = viscosity)	Temperature of glassy transition (°C)	Temperature of crystallization (°C)
F0	2.668 ± 0.002	7.2 ± 0.1	1273 ± 5	720 ± 5	935 ± 5
F1	2.857 ± 0.002	5.8 ± 0.1	1312 ± 5	800 ± 5	936 ± 5 and 1025 ± 5
F2	2.484 ± 0.002	2.8 ± 0.1	1365 ± 5	710 ± 5	890 ± 5 and 960 ± 5
F3	–	6.4 ± 0.1	–	750 ± 5	960 ± 5
F4	2.380 ± 0.002	12.8 ± 0.1	1310 ± 5	650 ± 5	885 ± 5
F5	2.630 ± 0.002	6.8 ± 0.1	1210 ± 5	505 ± 5	750 ± 5 and 1025 ± 5
F6	2.503 ± 0.002	7.1 ± 0.1	1330 ± 5	650 ± 5	955 ± 5

2. Experimental

Seven glass–ceramic systems (F0–F6) were selected among the most widely utilized by the ceramic industry (Table 1). They are prepared like ceramic frits, admixing the raw materials (oxides and carbonates) in almost stoichiometric proportions and adding small amounts of melting promoters [24,25]. These frits were characterized determining: bulk density (water pycnometry, ASTM C329), viscosity at high temperature (VEZAS), coefficient of thermal expansion (ASTM C 372), temperatures of glassy transition and crystallization (Table 2). Moreover the glass–ceramic systems underwent a thermal treatment, such as that of porcelain stoneware tiles, and the crystalline phases formed were determined (XRPD, Philips X'Pert Pro x, Cu Kα radiation, 10–80° 2θ range, 0.05° stepscan) (Table 1).

An industrial spray-dried powder (BR), made up of ball clays (37 wt.%) plus feldspars and quartz (63 wt.%), commonly employed for porcelain tile manufacture, was modified by adding the different frits; these latter were added in replacement (10 wt.%) of the non-plastic materials. The mineralogical composition of the industrial mixture BR is: 32.5 wt.% of kaolinitic and illitic clays, 31.2 wt.% of quartz, 30.8 wt.% of plagioclase and 5.5 wt.% of potassium feldspar.

The overall chemical composition of the frit-bearing bodies, from BF0 to BF6, is listed in Table 3 and compared with the reference one.

The simulation of the industrial tile-making process was carried out at laboratory scale by:

- mixing and wet grinding in porcelain jar with dense alumina grinding media for 20 min in a planetary mill (C.I. Magellano);
- slip drying at 105 ± 5 °C overnight, powder deagglomeration (by hammer mill, 0.75 mm grid) and humidification with 7–8% water;
- uniaxial pressing (40 MPa) of 110 mm × 55 mm × 6 mm tiles;
- drying in an electric oven at 105 ± 5 °C overnight;
- firing in an electric roller kiln (Nannetti, ER 15) at maximum temperature from 1200 °C up to 1240 °C with a thermal cycle of 51 min cold-to-cold.

Fired tiles were characterized by determining: firing shrinkage (ASTM C326), water absorption, bulk density (ρ_f) and open porosity (OP, ISO 10545-3), real density by helium pycnometry (ρ_r), total porosity ($TP = [1 - (\rho_f/\rho_r)] \times 100$), closed porosity ($CP = TP - OP$), CIE-Lab colourimetry (ISO 10545-16, Hunterlab MSXP-4000).

Table 3
Chemical composition (wt.%) of porcelain stoneware bodies

	BR	BF0	BF1	BF2	BF3	BF4	BF5	BF6
SiO_2	71.34	68.98	69.43	68.98	68.22	68.55	69.48	69.13
TiO_2	0.52	0.47	0.47	0.47	0.47	0.47	0.47	0.47
Al_2O_3	16.89	17.14	15.20	18.53	16.97	18.13	16.33	17.97
Fe_2O_3	0.56	0.50	0.50	0.50	0.50	0.50	0.50	0.50
MgO	0.47	1.35	0.42	2.12	0.42	0.42	1.13	0.42
CaO	0.56	2.85	3.64	0.50	0.50	0.62	2.20	0.69
Na_2O	4.02	3.61	3.61	3.61	3.61	5.52	3.61	4.28
K_2O	2.19	1.97	1.97	1.97	1.97	1.97	2.22	2.18
ZrO_2	–	–	1.64	–	–	0.17	0.93	0.26
ZnO	–	–	–	–	–	–	–	0.44
BaO	–	–	–	–	4.21	–	–	–
B_2O_3	–	–	–	–	–	0.50	–	0.43
Li_2O	–	–	–	0.20	–	–	–	0.09
P_2O_5	0.11	0.10	0.10	0.10	0.10	0.10	0.10	0.10
L.O.I.	3.34	3.00	3.00	3.00	3.00	3.00	3.00	3.00

Unfired tiles were characterized by measuring bulk density (BD, geometric method), specific weight (He pycnometry) and total porosity.

The sintering behavior was investigated by hot stage microscope (HSM, Expert System, Misura 3) measuring linear shrinkage in an industrial-like cycle as well as densification rates and expansion rate in isothermal condition (heating rate 80 °C/min to 1100, 1125, 1150, 1175 and 1200 °C). The apparent activation energy of densification was calculated according to Cho and Schulze [26] and Singh [27].

Quantitative phase composition analysis was performed on stoneware fired at 1220 °C (1240 °C for BF1 sample) by XRPD (Rigaku Miniflex, Cu Kα radiation, 10–80° 2θ range, 0.02° stepscan) adding 10 wt.% of Al_2O_3 (NIST 674) as internal standard and following a RIR-Rietveld procedure [28].

The chemical composition of the vitreous phase was inferred by phase and chemical composition of bulk stoneware; viscosity and surface tension of the liquid phase at high temperature were calculated with the equations of Lakatos et al. [29] and Cuartas [30], and Appen [31], respectively.

The microstructure of the graphite-coated polished surface of stoneware fired at 1200 °C (1240 °C for BF1) was investigated by SEM Leica Cambridge Stereoscan 360. The bulk chemical composition was checked by XRF-EDS (Link-Analytical electron microscope).

3. Results and discussion

3.1. Properties of glass–ceramic frits

The seven systems taken into account exhibit on the whole a wide range of physical properties, depending on the crystalline phases formed during devetrification and the complexity of the system. As shown in Table 1, there are simple ternary compositions (F3 and F4) giving rise to a single crystalline phase (plus residual glass), while other ternary systems (F1 and F2) are designed to produce composite materials. In addition, the quaternary system F0 and the two formulations F5 and F6 devetrify to a more complex assemblage of crystalline phases.

As reported in Table 2, these frits offer a wide set of bulk density values (2.380–2.857 g cm^{-3}), thermal expansion coefficients, with values ranging from 2.8 to 12.8 MK^{-1}, and different temperatures of vitreous transition (from 500 to 800 °C). The theoretical temperatures (Table 2), corresponding to log $\eta = 3$ (where η is the viscosity) and ranging from 1210 to 1365 °C, fit, for all systems, the gob temperatures of the ordinary basin kilns; moreover, the crystallization temperatures are in the useful window between melting and softening, in which the liquid phase viscosity is low enough to permit a structure rearrangement with minor residual stress [13–15].

3.2. Technological behaviour

The incorporation of glass–ceramic precursors into the porcelain stoneware body brings about a decreased bulk density of unfired tiles and a proportional increase of porosity from 31% (reference body) to 33–36% (frit-bearing bodies) (Table 4). This circumstance is a consequence of a minor powder flowability and green tile compactness when the glass–ceramic precursors replaced quartz–feldspathic fluxes. It is detrimental for green mechanical strength, but it is useful in most decorating techniques, involving glaze suspensions, soluble dyes, silk-screen pastes or ceramic inks that have to penetrate fast the porous substrate.

Table 4
Technological properties of semi-finished products

Bodies	Bulk density (g cm^{-3})	Total porosity (vol.%)
BR	1.80 ± 0.01	30.9 ± 0.1
BF0	1.73 ± 0.02	34.8 ± 0.1
BF1	1.73 ± 0.01	34.7 ± 0.1
BF2	1.72 ± 0.01	34.2 ± 0.1
BF3	1.69 ± 0.01	36.0 ± 0.1
BF4	1.65 ± 0.01	36.1 ± 0.1
BF5	1.74 ± 0.01	33.3 ± 0.1
BF6	1.71 ± 0.04	34.0 ± 0.1

The firing behaviour of porcelain stoneware tiles is heavily affected by the occurrence of glass–ceramic precursors (Table 5):

- Firing shrinkage is increased comparing the same thermal treatment or even the same degree of densification; this circumstance is to a large extent attributable to the porosity difference of unfired tiles, those containing frit being more porous (Fig. 1).
- Comparing tiles with a very low water absorption (i.e. ≅0.1%, as usually achieved in the industrial practice), the frit-bearing ones exhibit lower porosity and higher bulk density.
- Open, closed and total porosity for all bodies present about the same value at the temperature of maximum densification.
- The colour of frit-bearing tiles is significantly lighter (i.e. higher value of L^*) with negligible variations of the red (a^*) and yellow (b^*) components.

3.3. Phase composition

Glass–ceramic precursors induce remarkable changes in type, amount and chemistry of the crystalline and amorphous phases of porcelain stoneware. Each frit plays its own peculiar effect on phase composition. Anyway, some general trends may be outlined; in particular, vitreous precursors (Table 6):

- Promote the melting of quartz, whose amount in frit-bearing stoneware is reduced more than expected on the basis of the replacement of precursor after quartz raw materials.
- Do not significantly change the amount of mullite, except in the sample BF6 where it is more abundant; as a first hypothesis, the higher mullite content could be ascribed to the more favourable kinetics of the sintering process, as testified by the lowest value of the activation energy (E_a) and the fastest sintering rate.
- Let the glassy phase unchanged or slightly increased, apart from two extreme cases: BF0 has a relatively low content (58%), whereas BF2 has the larger amount of glass (76%).

Table 5
Technological properties of porcelain stoneware tiles

Body	Firing temperature (°C)	Firing shrinkage (cm m^{-1})	Water absorption (wt.%)	Open porosity (vol.%)	Closed porosity (vol.%)	Total porosity (vol.%)	Bulk density (g cm^{-3})	Colour CIE-Lab			
								L^*	a^*	b^*	ΔE^*
BR	1200	7.7 ± 0.1	1.75 ± 0.3	4.0 ± 0.7	4.6 ± 0.5	8.6 ± 0.9	2.299 ± 0.011	74.9 ± 0.1	3.1 ± 0.1	13.1 ± 0.1	Ref.
	1220	8.6 ± 0.1	0.09 ± 0.06	0.2 ± 0.1	3.4 ± 0.3	3.6 ± 0.4	2.394 ± 0.001	70.9 ± 0.1	2.6 ± 0.1	13.6 ± 0.1	Ref.
	1240	8.2 ± 0.1	0.09 ± 0.04	0.2 ± 0.1	3.6 ± 0.4	3.8 ± 0.4	2.375 ± 0.006	70.9 ± 0.1	2.2 ± 0.1	13.7 ± 0.1	Ref.
BF0	1200	8.8 ± 0.1	0.60 ± 0.02	1.4 ± 0.1	4.6 ± 0.5	6.0 ± 0.6	2.374 ± 0.003	73.5 ± 0.1	2.6 ± 0.1	14.6 ± 0.1	2.1 ± 0.1
	1220	9.4 ± 0.1	<0.01	<0.1	3.2 ± 0.3	3.2 ± 0.3	2.401 ± 0.003	73.1 ± 0.1	2.0 ± 0.1	15.3 ± 0.1	2.8 ± 0.1
BF1	1220	7.7 ± 0.1	0.55 ± 0.01	1.3 ± 0.1	5.8 ± 0.6	7.0 ± 0.7	2.335 ± 0.002	76.1 ± 0.1	1.7 ± 0.1	13.3 ± 0.1	5.3 ± 0.1
	1240	8.6 ± 0.1	0.09 ± 0.05	0.2 ± 0.1	3.1 ± 0.3	3.3 ± 0.3	2.386 ± 0.006	77.1 ± 0.1	1.3 ± 0.1	13.1 ± 0.1	6.3 ± 0.1
BF2	1200	9.7 ± 0.1	0.08 ± 0.04	0.2 ± 0.1	2.7 ± 0.3	2.9 ± 0.3	2.421 ± 0.007	73.2 ± 0.1	2.3 ± 0.1	13.4 ± 0.1	1.9 ± 0.1
	1220	9.6 ± 0.1	0.02 ± 0.09	0.1 ± 0.2	3.6 ± 0.4	4.0 ± 0.4	2.373 ± 0.006	74.7 ± 0.1	1.6 ± 0.1	13.4 ± 0.1	3.9 ± 0.1
BF3	1200	10.1 ± 0.1	2.66 ± 0.12	6.1 ± 0.2	4.4 ± 0.4	10.5 ± 1.0	2.285 ± 0.016	75.0 ± 0.1	2.8 ± 0.1	14.1 ± 0.1	1.0 ± 0.1
	1220	9.8 ± 0.1	0.07 ± 0.10	0.2 ± 0.3	3.2 ± 0.3	3.3 ± 0.3	2.436 ± 0.007	71.0 ± 0.1	2.5 ± 0.1	15.7 ± 0.1	2.1 ± 0.1
BF4	1200	8.2 ± 0.1	0.09 ± 0.04	0.2 ± 0.1	2.8 ± 0.3	3.0 ± 0.3	2.411 ± 0.006	71.4 ± 0.1	2.7 ± 0.1	14.3 ± 0.1	3.7 ± 0.1
	1220	10.7 ± 0.1	0.07 ± 0.03	0.2 ± 0.1	2.9 ± 0.3	3.1 ± 0.3	2.386 ± 0.021	72.6 ± 0.1	2.0 ± 0.1	14.8 ± 0.1	2.2 ± 0.1
BF5	1200	10.6 ± 0.1	0.54 ± 0.08	1.3 ± 0.2	5.2 ± 0.5	6.4 ± 0.6	2.411 ± 0.006	75.8 ± 0.1	2.2 ± 0.1	13.1 ± 0.1	1.3 ± 0.1
	1220	8.9 ± 0.1	0.11 ± 0.07	0.3 ± 0.2	4.0 ± 0.4	4.3 ± 0.4	2.386 ± 0.021	76.6 ± 0.1	1.6 ± 0.1	13.4 ± 0.1	5.8 ± 0.1
BF6	1200	8.6 ± 0.1	0.04 ± 0.06	0.1 ± 0.1	1.7 ± 0.2	1.8 ± 0.1	2.433 ± 0.020	72.8 ± 0.1	2.4 ± 0.1	12.8 ± 0.1	2.3 ± 0.1
	1220	9.7 ± 0.1	0.06 ± 0.08	0.1 ± 0.2	2.9 ± 0.3	3.0 ± 0.3	2.387 ± 0.010	74.0 ± 0.1	1.7 ± 0.1	13.1 ± 0.1	3.3 ± 0.1

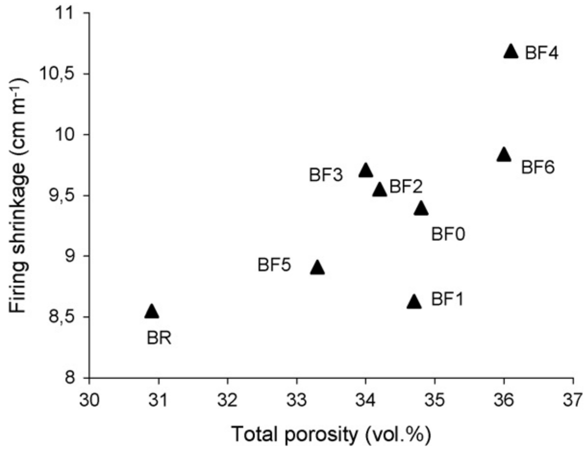

Fig. 1. Total porosity of unfired tiles vs. firing shrinkage at maximum densification.

- Slightly increase the amount of K-feldspar with the exception of the BF4 and BF6 bodies where the variations are negligible.
- Foster the stability of plagioclase in the samples BF0, BF1 and BF5 with respect to the reference body. This effect could be due to the persistence of more residual feldspar or the anorthite crystallization from CaO-rich systems, or both. In contrast, the plagioclase is completely melted in the sample BF2.

Table 7
Chemical and physical properties of the glassy phase calculated at maximum densification

	BR	BF0	BF1	BF2	BF3	BF4	BF5	BF6
SiO_2 (wt.%)	70.4	66.8	69.0	67.5	67.7	67.3	67.8	68.7
TiO_2 (wt.%)	0.8	0.8	0.7	0.6	0.7	0.7	0.7	0.7
ZrO_2 (wt.%)	–	–	2.5	–	–	0.2	1.5	0.4
Al_2O_3 (wt.%)	18.1	18.3	15.2	20.4	17.5	19.3	16.9	17.4
B_2O_3 (wt.%)	–	–	–	–	–	0.7	–	0.6
Fe_2O_3 (wt.%)	0.9	0.9	0.7	0.7	0.8	0.7	0.8	0.8
ZnO (wt.%)	–	–	–	–	–	–	–	0.7
BaO (wt.%)	–	–	–	–	4.8	–	–	–
MgO (wt.%)	0.7	2.4	0.6	2.8	0.6	0.6	1.8	0.6
CaO (wt.%)	0.9	5.1	5.5	0.7	0.8	0.9	3.6	1.0
Li_2O (wt.%)	–	–	–	0.3	–	–	–	0.1
Na_2O (wt.%)	5.3	3.2	3.4	4.9	4.7	7.1	3.7	6.0
K_2O (wt.%)	3.1	2.5	2.4	2.1	2.4	2.5	3.0	2.9
Viscosity (kPa s) [29]	2.7	2.8	n.d.	3.2	2.3	2.5	2.4	2.1
Viscosity (kPa s) [30]	4.2	3.6	n.d.	5.1	4.5	4.0	3.6	3.6
Surface tension ($mN\ m^{-1}$) [31]	327	345	334	340	328	383	354	353

During the firing cycle of porcelain stoneware, only some frits behave as a real glass–ceramic material: the sample BF3 gives rise to the formation of celsian and the body BF1 generates calcium zirconium silicate. Moreover, in both BF1 and BF5 zircon was formed. These findings are confirmed by SEM observations (Fig. 2).

Table 6
Phase composition of porcelain stoneware tiles

Body	Firing temperature (°C)	Quartz	K–feldspar	Plagioclase	Mullite	Celsian	Zircon	Calcium zircosilicate	Amorphous phase
BR	1220	20.5 ± 0.2	1.2 ± 0.2	5.3 ± 0.4	5.7 ± 0.3	–	–	–	67.3 ± 1.0
BF0	1220	18.0 ± 0.1	3.4 ± 0.2	15.7 ± 0.3	4.7 ± 0.3	–	–	–	58.2 ± 0.9
BF1	1240	13.7 ± 0.4	2.5 ± 0.5	11.8 ± 0.4	3.5 ± 0.2	–	0.5 ± 0.1	1.9 ± 0.4	66.1 ± 2.0
BF2	1220	16.8 ± 0.3	2.8 ± 0.1	$<0.5 \pm 0.1$	4.4 ± 0.3	–	–	–	76.0 ± 0.8
BF3	1220	17.3 ± 0.3	2.7 ± 0.1	4.8 ± 0.1	5.0 ± 0.5	3.2 ± 0.3	–	–	67.0 ± 1.0
BF4	1220	16.4 ± 0.1	1.5 ± 0.3	5.0 ± 0.2	5.0 ± 0.2	–	–	–	72.1 ± 0.8
BF5	1220	17.9 ± 0.2	2.2 ± 0.3	11.7 ± 0.3	4.8 ± 0.2	–	0.5 ± 0.1	–	62.9 ± 1.0
BF6	1220	19.2 ± 0.1	1.3 ± 0.1	2.3 ± 0.3	8.1 ± 0.2	–	–	–	69.1 ± 0.7

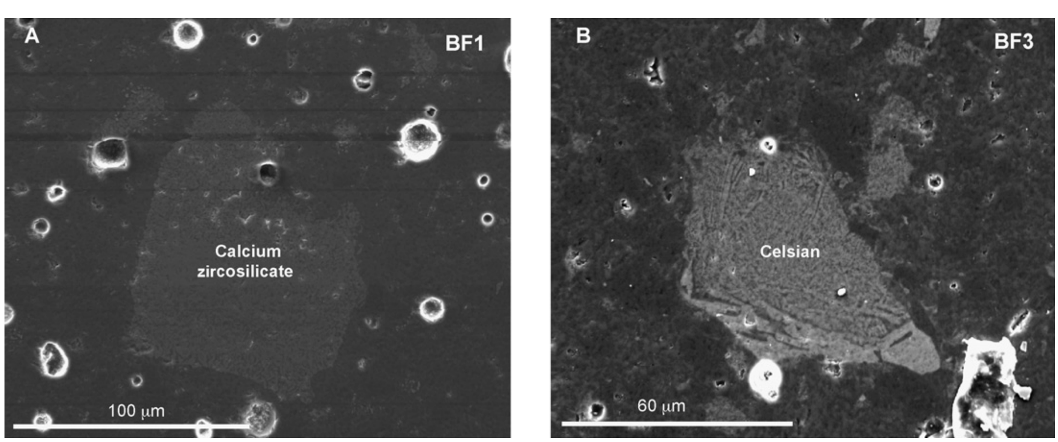

Fig. 2. SEM micrographs of the samples: (A) BF1 (ZCS) fired at 1240 °C and (B) BF3 (BAS) fired at 1220 °C.

In the other systems, which do not promote the crystallization of new phases, the main components (i.e. CaO, MgO, Na_2O, K_2O, ZnO) are diffused into the liquid phase, altering the most important physical factors contributing to densification (i.e. viscosity and surface tension). The addition of frits produced noticeable changes in the chemical composition of the liquid phase (Table 7); in particular, the samples containing a glass–ceramic precursor, if compared to the reference body, shows:

- Decreasing SiO_2 concentration, due to a large extent to lower silica amount in the initial mix.

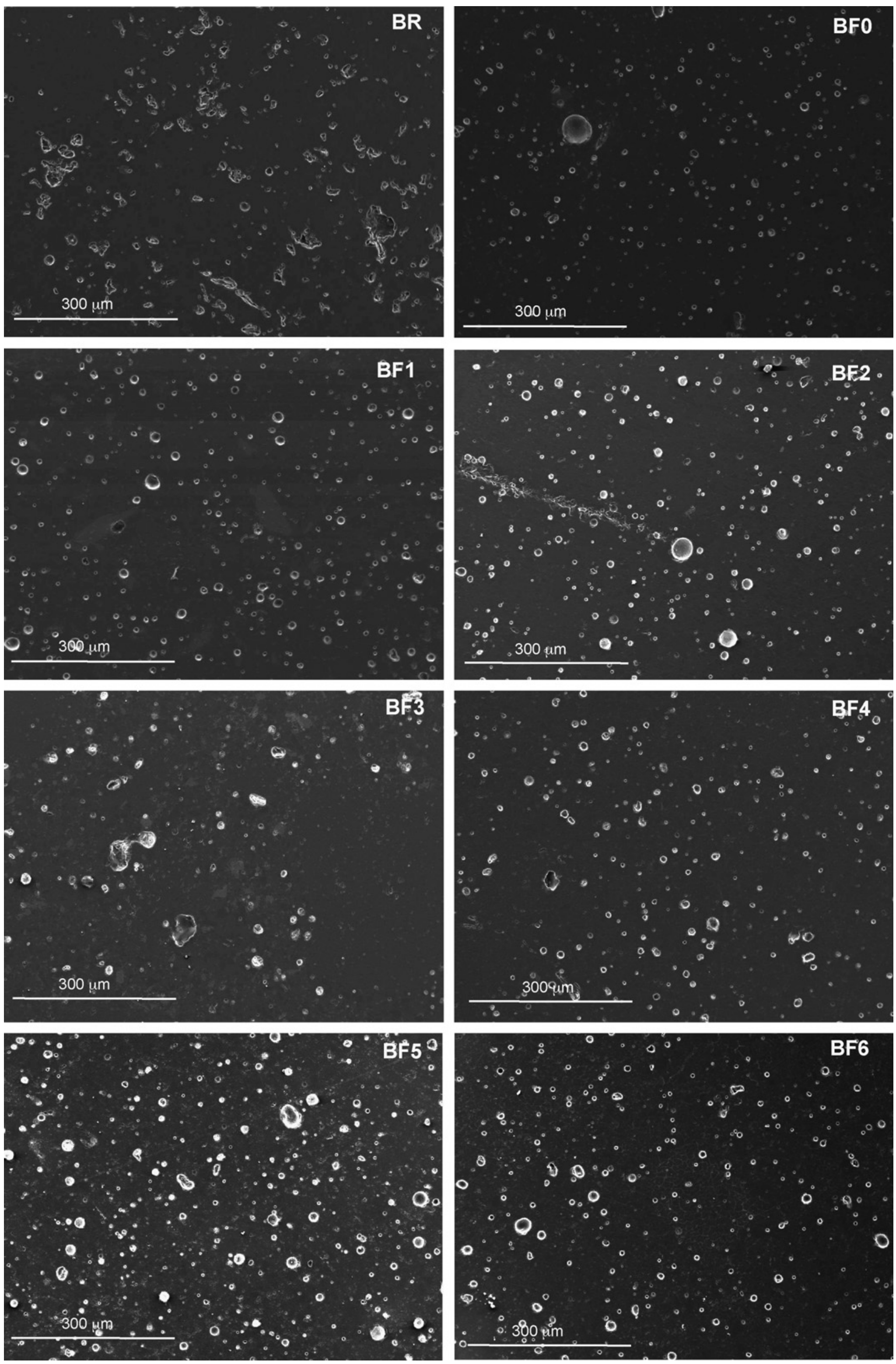

Fig. 3. SEM micrographs of the bodies, fired at 1220 °C, but BF1 at 1240 °C.

- Similar Al_2O_3 values, with the exception of BF1 where there is a conspicuous drop.
- Decrease of Na_2O and K_2O contents, but in the bodies BF4 and BF6, where an increase of sodium occurred, due to the Na_2O contribution by the NAS and CZNAS precursors.
- Increase of CaO and/or MgO (BF0, BF1, BF2, BF5) related to the addition of CMAS, ZCS, MAS, and MAKCZS systems, respectively.
- Occurrence of significant amounts of BaO (BF3) and ZrO_2 (BF1, BF5) partially dissolved in the liquid phase.

The physical properties of the glassy phase, summarized in Table 7, vary according to the chemical composition of glass–ceramic frits. The surface tension of liquid phase, indicating its wetting capacity, is raised by the glass–ceramic frit additions whereas viscosity is generally decreased. Viscosity was determined by two different empirical approaches proposed by Lakatos et al. [29] and Cuartas [30], which where set up for the soda-lime glass composition ranges. The composition of our samples differs from that considered in these models for higher alumina amounts and the occurrence of ZrO_2. This latter makes somewhat unreliable the prediction concerning the sample BF1. Even the prediction of MgO-rich liquid phases is somewhat doubtful, resulting in an increased viscosity that is against experimental observations [32].

3.4. Microstructure

The microstructure of samples fired at 1220 °C (or 1240 °C for the body BF1) is shown in Fig. 3. At this temperature, all bodies present about the same values of total porosity (3–4 vol.%), as also confirmed by the results of Table 5, with a very low fraction (0.1–0.3 vol.%) belonging to open porosity; however, looking more in detail at the micrographs of Fig. 3, a different number of pores having a more or less regular morphology is present and some quite evident differences come out:

(i) in the reference sample BR at 1220 °C there is the presence of a great number of pores with irregular morphology;
(ii) the amount of pores seems to increase when glass–ceramic frits are present and this effect is particularly evident in the samples BF5 and BF6;
(iii) the pore size of the added bodies BF1–BF6 seems to be lower and with a more spherical shape, when compared to the reference one BR.

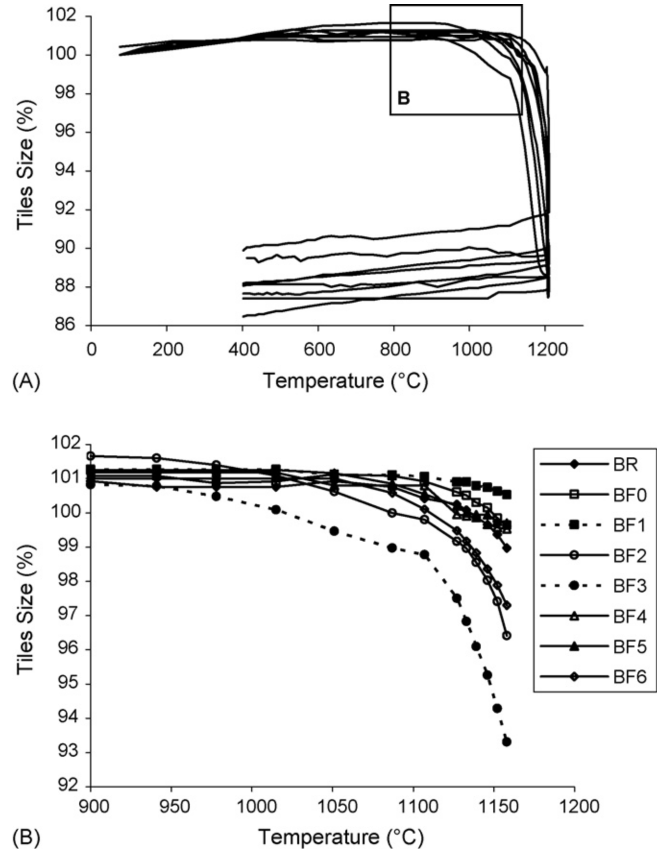

Fig. 4. Firing behaviour of porcelain stoneware bodies in an industrial-like cycle.

3.5. Sintering behaviour

Constant rate thermodilatometry, showing the dimensional variations as a function of temperature (Fig. 4), indicates that

Table 8
Shrinkage, sintering rate, coarsening rate and apparent energy of activation of the viscous flow in the porcelain stoneware tiles

Parameter	Temperature (°C)	Sample							
		BR	BF0	BF1	BF2	BF3	BF4	BF5	BF6
Linear shrinkage at maximum densification (cm m^{-1})	1100	4.7	2.8	0.2	10.5	1.8	5.4	2.2	7.3
	1125	7.7	7.5	2.0	11.7	4.8	11.3	5.7	12.0
	1150	5.6	13.6	4.8	11.4	11.6	11.9	11.2	11.6
	1175	9.4	10.7	9.5	11.3	11.6	11.7	11.1	11.3
	1200	9.4	11.4	11.3	10.8	12.3	11.6	11.1	10.7
Sintering rate (min^{-1})	1200	4.7	6.0	1.7	6.8	5.7	5.7	5.3	7.7
Coarsening rate (min^{-1})	1200	3.9	9.9	<0.1	17.3	5.3	11.4	11.3	9.3
Apparent energy of activation, E_a (kJ mol^{-1})		770	938	1824	568	637	941	467	297
Temperature of onset of densification (°C)		1130	1130	1130	980	980	1050	1090	1090

the body densification by viscous flow starts at different onset temperatures (TOD). The reference body BR begins to density at about 1130 °C (Table 8), while the frit-containing samples start at the same or at lower temperatures (Fig. 4B), despite the lower bulk density of green compacts. The onset temperature exhibits a poor correlation with the apparent energy of activation of viscous flow, in contrast with expectations, the relationship being made complex by the different green densities.

The sintering rate of porcelain stoneware tiles was measured on the isothermal curves (from 1120 to 1200 °C) shown in Fig. 5, where the dimensional variations have been contrasted with the elapsed time. This rate is somehow affected by the different typology of glass–ceramic frits: at 1200 °C, which is the typical industrial firing temperature of porcelain stoneware, almost all samples reach the maximum densification in a few minutes. Generally, the shrinkage values are between 5 and 9%, but for the system BF1 whose rate is slower. The sintering rate

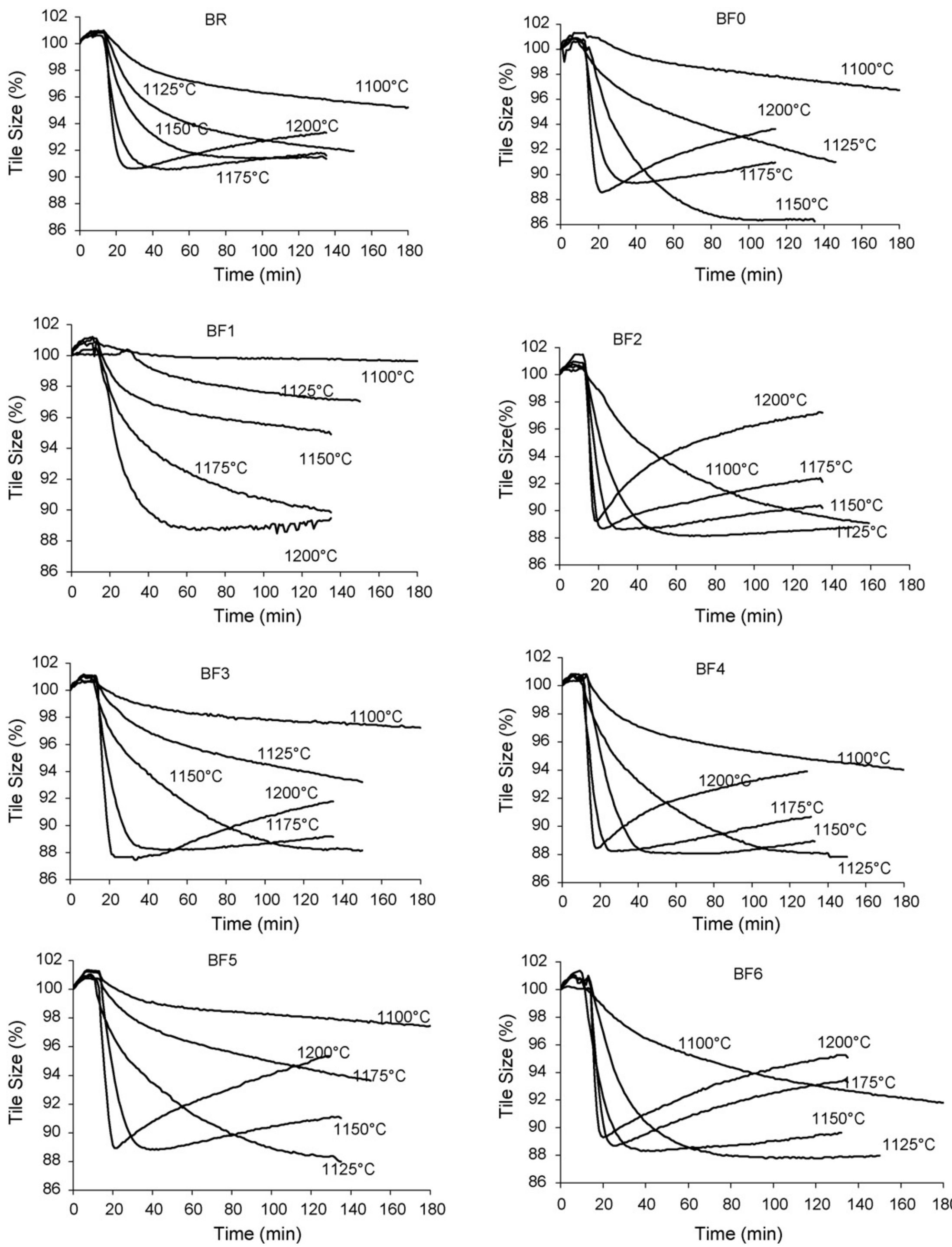

Fig. 5. Isothermal sintering curves of porcelain stoneware bodies.

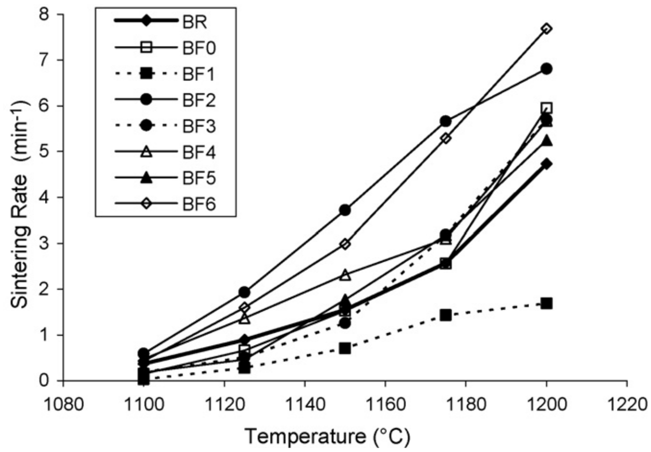

Fig. 6. Sintering rate vs. temperature of isothermal treatment.

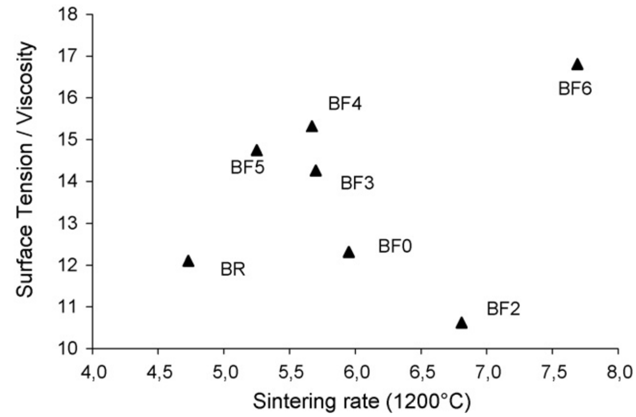

Fig. 8. Sintering rate (1200 °C) vs. the surface tension-to-viscosity ratio at the maximum densification.

is enhanced by the glass–ceramic additions, particularly when the F2 and F6 systems are used (Fig. 6); the only exception being again the sample BF1.

The value of shrinkage at maximum densification increases regularly from 1100 to 1200 °C for all samples (Table 8). The exceptions are the fast-sintering bodies BF2 and BF6 that shrink less at the highest temperature due to an overfiring effect.

The addition of glass–ceramic frit causes a clear modification of the apparent energy of activation of the viscous flow, that ranges from 297 to 1824 kJ mol^{-1} (Table 8). Moreover, the lower the energy to begin densification, the faster the sintering rate (Fig. 7).

According to models of sintering by viscous flow of glass, such as the Frenkel's and the Mackenzie-Shuttleworth's ones [33,34], the sintering rate depends directly on the surface tension and inversely on the viscosity of the liquid phase at the firing temperature. A certain positive correlation of the surface tension-to-viscosity ratio does exist with the sintering rate, apart the MAS-bearing BF2 body (Fig. 8). This sample is characterized by a liquid phase rich in MgO, which the models used to calculate the viscosity attribute the role of increasing viscosity, that is some how in contrast with evidences of sintering promoter of magnesium [32].

The coarsening rate (Table 8) is clearly increased with the addition of glass–ceramic frits, except the body BF1, where the ZCS system avoided any bloating. A similar effect, though less evident, occurred in the body BF3. However, the microstructure of the samples fired at 1220 °C does not show any evident coarsening; only a larger number of pores occurs in the bodies BF5 and BF6, but no pore growth is observed (Fig. 3). It is

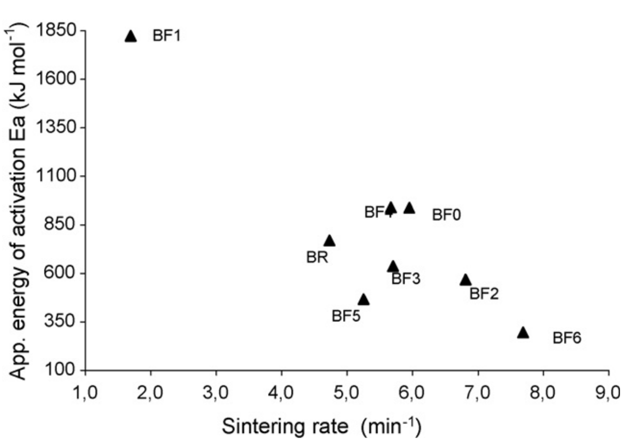

Fig. 7. Sintering rate (1200 °C) vs. apparent energy of activation.

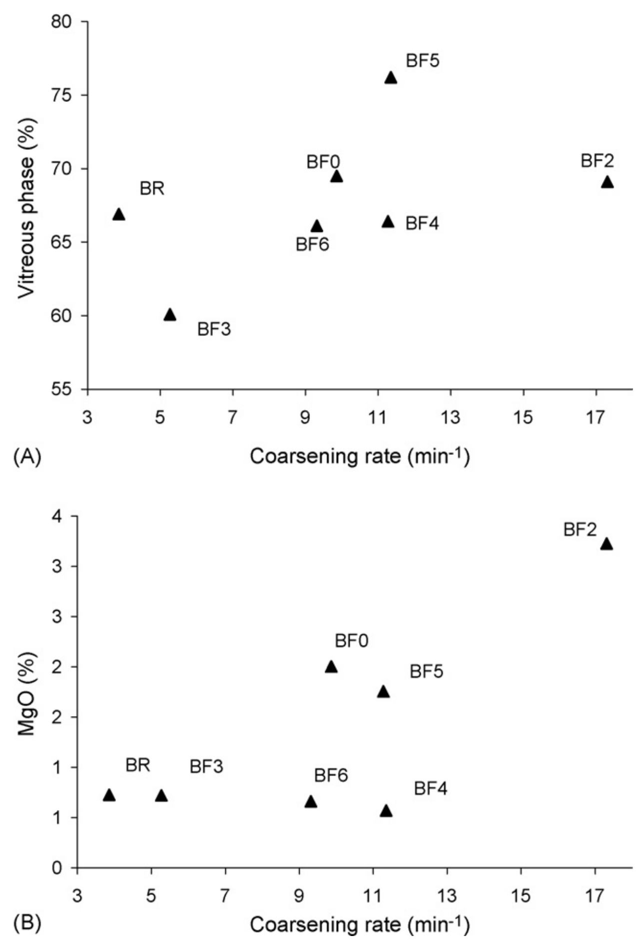

Fig. 9. Coarsening rate (1200 °C) vs. the amount of glassy phase (A) and MgO in the liquid phase (B) at maximum densification.

possible that the coarsening phenomenon will appear after treatment at higher temperature or longer cycles. Overall, the coarsening rate appears to depend on both the amount of glassy phase and the percentage of MgO in the liquid phase (Fig. 9).

4. Conclusions

The addition of glass–ceramic frits as fluxing raw materials is able to improve both the technical performance and aesthetical properties of porcelain stoneware tiles.

The glass–ceramic systems currently used in the manufacture of porcelain stoneware tiles significantly affect the composition, technological and aesthetical properties of the bodies; in any case, the technological and mechanical performances of bodies containing glass–ceramic precursors are equal or better than reference industrial batches.

The addition of glass–ceramic precursor is detrimental for the compactness of the green body, but the consequently enhanced porosity and permeability are very useful in decoration purposes, involving the fast absorption of glaze suspensions, soluble dyes, silk-screen pastes or ceramic inks.

The standard target of water absorption ($\cong$0.1%) for porcelain stoneware tiles is accomplished at the same firing temperature also with the frit additions, but with an exception for the system $CaO–ZrO_2–SiO_2$ (F1). No substantial changes of residual porosity and bulk density occurred, though the firing shrinkage increases to up to 2%, due to a large extent to the higher porosity of green tiles. The microstructure of the samples at maximum densification is affected by glass–ceramic precursors, leading to pores characterized by a spherical shape.

The colour of frit-bearing tiles is significantly lighter than the reference body; this implies a better chromatic yield of ceramic pigments in through-body applications and consequently a much lower cost to obtain a determined colour intensity.

However, each frit plays its own peculiar effect in the compositional properties and only some precursors behave as real glass–ceramic materials, giving rise to the formation of celsian (BF3) and calcium zirconium silicate (BF1). The use of other glass–ceramic systems brought about the increase of the vitreous phase (BF2–BF4–BF5) or the occurrence of large amounts of feldspar (BF0–BF1–BF5). The components of the frits, mainly alkaline and alkaline-earth oxides, are diffused into the liquid phase, altering the most important physical properties (viscosity and surface tension) for densification. The positive influence of the glass–ceramic additions in promoting the sintering stands out when the onset temperature of densification and the sintering rate are concerned: both are improved with respect to the reference body. In particular, the sintering rate of porcelain stoneware tiles depends on the properties of the liquid phase at high temperature (i.e. surface tension/viscosity ratio).

The coarsening rate appears to depend on both the amount and composition of liquid phase, being the percentage of MgO determinant to foster bloating phenomena.

References

[1] T. Manfredini, L. Pennisi, G. Pellacani, M. Romagnoli, Porcelanized stoneware tile, Am. Ceram. Soc. Bull. 74 (1995) 76–79.
[2] M. Dondi, B. Fabbri, T. Manfredini, G.C. Pellacani, Microstructure and mechanical properties of porcelanized stoneware tiles, in: Proceedings of the Fourth European Ceramics, vol. 11, 1995, pp. 319–326.
[3] C. Leonelli, P. Veronesi, V. Cannillo, G.C. Pellacani, A.R. Boccaccini, Porcelanized stoneware as a composite material: identification of strengthening and toughening mechanisms, Tile Brick Int. 17 (2001) 238–245.
[4] M. Dondi, G. Ercolani, M. Marsigli, C. Melandri, C. Mingazzini, The chemical composition of porcelain stoneware tiles and its influence on microstructure and mechanical properties, Interceram 48 (2) (1999) 75–83.
[5] C. Leonelli, F. Bondioli, P. Veronesi, M. Romagnoli, T. Manfredini, G.C. Pellacani, V. Cannillo, Enhancing the mechanical properties of porcelain stoneware tiles: a microstructural approach, J. Eur. Ceram. Soc. 21 (2001) 785–793.
[6] A.L. Costa, G. Cruciani, M. Dondi, F. Matteucci, New outlooks on ceramic pigments, Ind. Ceram. 23 (1) (2003).
[7] G. Baldi, E. Generali, D. Settembre Blundo, Preparazione, caratterizzazione ed applicazione industriale di un vetroceramico appartenente al sistema $ZrO_2–CaO–SiO_2$ (ZCS) come componente in impasti da gres porcellanato, Ceramurgia 30 (2000) 161–171.
[8] F.J. Torres, J. Alarcòn, Pyroxene-based glass–ceramics as glazed for floor tiles, J. Eur. Ceram. Soc. 25 (2005) 349–355.
[9] F.J. Torres, E.R. De Sola, J. Alarcòn, Effect of some additives on the development of spinel-based glass–ceramic glazes for floor-tile, J. Non-Crystal. Solids 351 (2005) 2453–2461.
[10] G. Baldi, E. Generali, C. Leonelli, T. Manfredini, G.C. Pellacani, C. Siligardi, Effect of nucleating agents on diopside crystallization in new glass–ceramics for tile-glaze application, J. Mater. Sci. 30 (1995) 3251–3255.
[11] L. Barbieri, C. Leonelli, T. Manfredini, Technological and product requirements for fast firing glass–ceramic glazes, Ceram. Eng. Sci. Proc. 17 (1996) 11–22.
[12] A.M. Ferrari, L. Barbieri, C. Leonelli, T. Manfredini, C. Siligardi, C. Corradi, Feasibility of using cordierite glass–ceramics as tile glazes, J. Am. Ceram. Soc. 80 (1997) 1757–1766.
[13] T. Manfredini, C. Leonelli, I materiali vetroceramici: struttura, proprietà ed applicazioni. Parte I. Aspetti teorici, Ceram. Inform. 389 (1999).
[14] P. Knott, The glassy state Interceram, Ceram. Monogr. Suppl. 32 (6) (1983).
[15] T. Manfredini, C. Leonelli, I materiali vetroceramici: struttura, proprietà ed applicazioni. Parte II. Aspetti applicativi, Ceram. Inform. 398 (2000).
[16] W. Pannhorst, Glass ceramics: state-of-the-art, J. Non-Crystal. Solids 219 (1997) 198–204.
[17] C. Siligardi, C. Leonelli, G. Baldi, E. Generali, Studio di sinterizzazione di polveri di fritte vetro-ceramiche, Ceram. Inform. 393 (1999).
[18] C. Siligardi, M.C. D'Arrigo, C. Leonelli, Sintering behaviour of glass–ceramic frits, Am. Ceram. Soc. Bull. 79 (9) (2000).
[19] V. Biasini, M. Dondi, S. Guicciardi, C. Melandri, M. Raimondo, E. Generali, D.S. Blundo, Mechanical properties of porcelain stoneware tiles: the effect of glass ceramic system, Key Eng. Mater. 206–213 (2002) 1799–1802.
[20] G. Baldi, E. Generali, L. Rovatti, D.S. Blundo, Applicazioni di sistemi vetroceramici nefelinici quali promotori di sinterizzazione in impasto di gres porcellanato smaltato: I^a–II^a parte, Ceram. Inform. 415–420 (2002).
[21] G. Baldi, D. Biserni, E. Generali, D. Mazzini, D.S. Blundo, Il gres vetroceramico: aspetti scientifici e tecnologici di una nuova classe di materiali, Ceram. Inform. 396 (2000).
[22] L. Barbieri, A. Corradi, I. Lancellotti, T. Manfredini, Use of municipal incinerator botton ash as sintering promoter in industrial ceramics, Waste Manage. 22 (2002) 859–863.
[23] F.J. Torres, J. Alarcòn, Effect of MgO/CaO ratio on the microstructure of cordierite-based glass–ceramic glazes for floor tiles, Ceram. Int. 31 (2005) 683–690.

[24] A. Moreno, J. Garcia-Ten, J. Cabedo, R. Berge, J. Colom, Feasibility of using frits as raw materials in porcelain tile compositions, in: Proceedings of the Congress QUALICER, 2000, pp. 465–473.
[25] M.T. Tichell, J. Sànchez, I. Nebol-Diaz, Glass-ceramic glazes with aluminate and alumino silicate crystallisations adapted to porcelain tile bodies, in: Proceedings of the Congress QUALICER, 2000, pp. 237–251.
[26] Y.S. Cho, W. Schulze, Crystallization kinetics and properties of non-stoichiometric cordierite based thick film dielectrics, J. Am. Ceram. Soc. 82 (11) (1999) 3186–3192.
[27] V.K. Singh, Sintering of calcium alluminate mixes, Br. Ceram. Trans. 98 (4) (1999) 187–191.
[28] A.F. Gualtieri, Accuracy of XRPD using the combined Rietveld-RIR method, J. Appl. Crystallogr. 33 (2000) 267–278.
[29] T. Lakatos, G. Johansson, B. Skimmingskold, Viscosity temperature relations in the glass system SiO_2–Al_2O_3–Na_2O–K_2O–CaO–MgO in the composition range of technical glasses, Glass Technol. 13 (1972) 88–95.
[30] R.R. Cuartas, Calculo teorico de propriedades del vidrio: viscosidad, parametros termicos y parametros de desvitrificacion, Bol. Soc. Esp. Ceram. Vidrio 23 (2) (1984) 105–111.
[31] F. Cambier, A. Leriche, Vitrification, in: R.W. Cahn, P. Haasen, E.J. Kramer (Eds.), Materials Science Technology: A Comprehensive Treatment. Part II. Processing of Ceramics, vol. 17B, VCR Verlagsgesellschaft, Weinheim, 1996 , pp. 123–144 (chapter 15).
[32] M. Dondi, V. Biasini, G. Guarini, M. Raimondo, A. Argnani, S. Di Primio, Effect of talc and chlorite on sintering and technological behaviour of porcelain stoneware tiles, Silic. Ind. 68 (5–6) (2003) 67–73.
[33] E.D. Zanotto, M.O. Prado, Isothermal sintering with concurrent crystallisation of monodispersed and polydispersed glass particles. Part 1, Phys. Chem. Glass 42 (2001) 191–198.
[34] M.O. Prado, C. Federicci, E.D. Zanotto, Glass sintering with concurrent crystallisation. Part 2. Non-isothermal sintering of jagged polydispersed particles, Phys. Chem. Glass 43 (2002) 1–9.